Texas Transportation Institute
The Texas A&M University System
3135 TAMU
College Station, TX 77843-3135

979-845-6375
Fax: 979-845-6107
http://tti.tamu.edu

TECHNICAL MEMORANDUM

Contract No.: **405160-7**
Report No.: **405160-7-1**
Project Name: **Guidelines for W-beam Guardrail Post Installation in Rock**
Sponsor: **Roadside Safety Research Program Pooled Fund TPF-5(114)**

DATE: **May 29, 2009**

TO: **Dave Olson**
Policy, Standards and Safety Research Manager, Washington State Department of Transportation

COPY TO: Jesus Palomo, TTI RDO
D. L. Bullard, Jr., Head, Safety & Structural Systems
Rebecca Haug, TTI Safety & Structural Systems

FROM: **Nauman M. Sheikh**, Associate Transportation Researcher, TTI
Roger P. Bligh, Research Engineer, TTI
Wanda L. Menges, TTI Proving Ground

FOR MORE INFORMATION:
Name: Nauman M. Sheikh
Phone: (979)-845-8955
Email: nauman@tamu.edu

SUMMARY REPORT:

Introduction

A W-beam guardrail system requires that posts used to support the guardrail be installed at a certain minimum depth for proper functioning of the guardrail. In 1987, Hirsh and Beggs conducted research on the use of W-beam guardrails on low-fill bridge length culverts, where the soil-fill depth over the culverts was not enough to achieve full embedment depth of the guardrail posts [*1*]. Two crash tests were conducted with seven consecutive wooden posts in the impact region installed at embedment depths of 457 mm (18 inches) and 686 mm (27 inches), respectively. Both tests were unsuccessful. It was concluded that sufficient embedment depth was needed for proper functioning of the W-beam guardrail.

It is not always easy obtain the required embedment depth for posts in the field. One common situation is when rock is encountered at the surface or some depth below the

surface, preventing the installation of the post at the required embedment depth. Thus guidance is needed for installation of guardrail posts in such scenarios.

In 2003, Herr et al. developed a W-beam guardrail system for installation in rock-soil foundation [2]. In a crash test, the W152×13.4 (W6×8.5) steel posts were installed in concrete (to simulate rock) by drilling three overlapping 203 mm (8-inch) diameter holes that were 165 mm (6.5-inch) apart at their centers and were 610 mm (24 inches) deep. The holes were backfilled with compacted ASTM C33 coarse aggregate. The system was successfully tested for National Cooperative Highway Research Program (NCHRP) *Report 350* at Test Level 3. The researchers conducted some further bogie testing of guardrail posts and recommended that when guardrail posts are placed in rock, a 533 to 584 mm (21 to 23-inch) diameter elongated hole be cored and backfilled with crushed stone aggregate. This allowed the post to rotate and deflect under vehicular impact. The elongated hole is achieved by coring three partially overlapping 203 mm (8-inch) diameter holes. Alternately, a single larger diameter hole could be drilled for installation of the post. Due to the suggested coring requirements, the W-beam installation in rock becomes very expensive and may not be practical in many locations.

Objective

The objective of this research was to develop cost effective guidelines for placement of W-beam guardrail posts in rock by optimizing current placement guidelines and by investigating the sensitivity of W-beam guardrail performance to post embedment depth. The guidelines were to be developed for *NCHRP Report 350* evaluation criteria.

Research Approach

The researchers evaluated the existing guidelines for coring in rock and performed a geometric optimization with the objective of reducing some of the coring requirements. The greater focus of this research however was on evaluating the W-beam guardrail performance to develop guidelines that would eliminate or reduce the coring requirements. Due to funding limitations, it was proposed to conduct this research in two phases. In the first phase (documented herein), preliminary guidelines would be developed based on simulation analyses aimed at evaluating the W-beam guardrail performance when one or more posts are missing or installed at reduced embedment depth due to the presence of rock. The preliminary guidelines developed through simulation would identify various combinations of reduced post embedment depths or missing posts that would be expected to result in acceptable performance of the W-beam guardrail. Identifying such combinations would allow greater flexibility in installing W-beam guardrail posts when rock is encountered.

At the end of the first phase, the participating states of the pooled-fund research were to review the preliminary guidelines. If the states find the guidelines suitable, a second phase would be funded through the pooled-fund for verifying the guidelines through full-

scale crash testing. Based on the results of the crash testing, the preliminary guidelines may be modified to develop the final guidelines for installing guardrail posts in rock.

The benefit of adopting this research approach is that it provides greater understanding of when coring in rock is or is not required. Additionally, when coring is necessary, the new guidelines would suggest an optimized hole configuration yielding minimum coring depth. The details of various tasks performed are presented next.

Geometric Optimization of Existing Guidelines

The existing guidelines for installing W-beam guardrail post in rock were developed by the Midwest Roadside Safety Facility (MwRSF) [2]. The guidelines present an elongated hole configuration that is cored into the rock for post installation. The elongated hole is achieved by drilling three overlapping holes in the rock. After setting the post, the hole is backfilled with compacted coarse aggregate. This arrangement allows the post to rotate and deflect under vehicular impact. Depending on the depth at which the rock is encountered, the depth of the elongated hole may vary from 530 mm to 203 mm (21 inches to 8 inches) (see figure A-1 of Attachment A).

Federal Highway Administration (FHWA) issued a memorandum in 2004 for guidance on guardrail post installation in rock. The memorandum was based on the research conducted at MwRSF [3]. It was a simplified version of the MwRSF guidelines and reduced the number of scenarios presented in the original MwRSF version. Due to the difficulties that may arise in drilling the elongated hole, the revised version also allowed drilling a single larger diameter hole in lieu of the elongated hole (see figure A-2).

Since MwRSF's original guideline contained more scenarios depending on the range of depths at which the rock was encountered, and because some of these scenarios reduced the amount of drilling compared to the simplified version of the FHWA memorandum, the researchers evaluated the original MwRSF guidelines in this research.

In the bogie testing performed by MwRSF to evaluate the post response in compacted coarse aggregate, the post was found to deflect rigidly in the aggregate. Therefore, for the purpose of geometric optimization of the existing guidelines, only rigid-body rotation of the post was considered. Results of the geometric optimization are shown in figure A-3 of Attachment A.

It was determined that the geometric optimization of the existing guidelines does not render significant savings in the drilling requirements. In only one of the cases presented in the guidelines could the drilling of the third overlapping hole (to form the elongated hole) be reduced by 282 mm (11 inches) as shown in figure A-4. If an elongated hole cannot be achieved in the field, or the states have a preference for drilling a single larger diameter hole, this saving cannot be achieved.

Evaluation of W-Beam Guardrail with Missing or Reduced-Embedment Posts

Pendulum Testing

To provide data for evaluation of the performance of the W-beam guardrail system when some of the posts are either missing or installed at reduce embedment due to the presence of rock, the researchers performed a series of pendulum tests of soil embedded posts. In these tests, wood and steel posts were installed at various embedment depths. The posts were then impacted by a gravitational pendulum to measure the acceleration-time response resulting from the impact. This enabled the researchers to quantify the post-and-soil interaction behavior at various embedment depths. Details of the pendulum testing are presented in Attachment B.

Simulation Analysis

The researchers then performed a program of simulation analyses that was divided into three phases as follows.

1. Develop finite element model of the pendulum tests with posts embedded at various depths. Calibrate soil material properties in the model to adequately capture the post-soil interaction observed for posts installed at varying embedment depths.
2. Develop full-scale finite element model of the W-beam guardrail system using the post-soil model. Validate results of the model using previously conducted crash tests of the W-beam guardrail system.
3. Perform a parametric evaluation of the W-beam guardrail performance when one or more posts are missing or are at reduced embedment due to the presence of rock. The finite element model of the W-beam guardrail system would be used in this parametric analysis along with the post-soil models developed for reduced post embedment depths.

The objective of the parametric analysis was to determine if a particular combination of reduced embedment and/or missing posts would "pass" or "fail" under NCHRP Report 350 testing criteria. Based on these results, the preliminary guidelines for W-beam post installation in rock would be developed. For combinations where the guardrail performance is found acceptable, no coring in the rock would be necessary, even when some of the posts are not installed at full embedment depth. For other combinations, some coring may still be required to achieve acceptable performance of the W-beam guardrail. Using this approach would presumably require less frequent drilling in the rock and provide a much greater flexibility in installing W-beam guardrail in rock.

Post-Soil Modeling

After the pendulum testing, the researchers developed component level finite element models of the guardrail post in soil at various embedment depths. The posts were impacted with a gravitational pendulum model as in the test (see figure 1). The soil

material was initially modeled using the Geologic Cap material model (MAT 25) in LS-DYNA. Starting with standard soil material properties, a parametric calibration of the soil properties was performed to match the post-soil interaction behavior between simulation and testing.

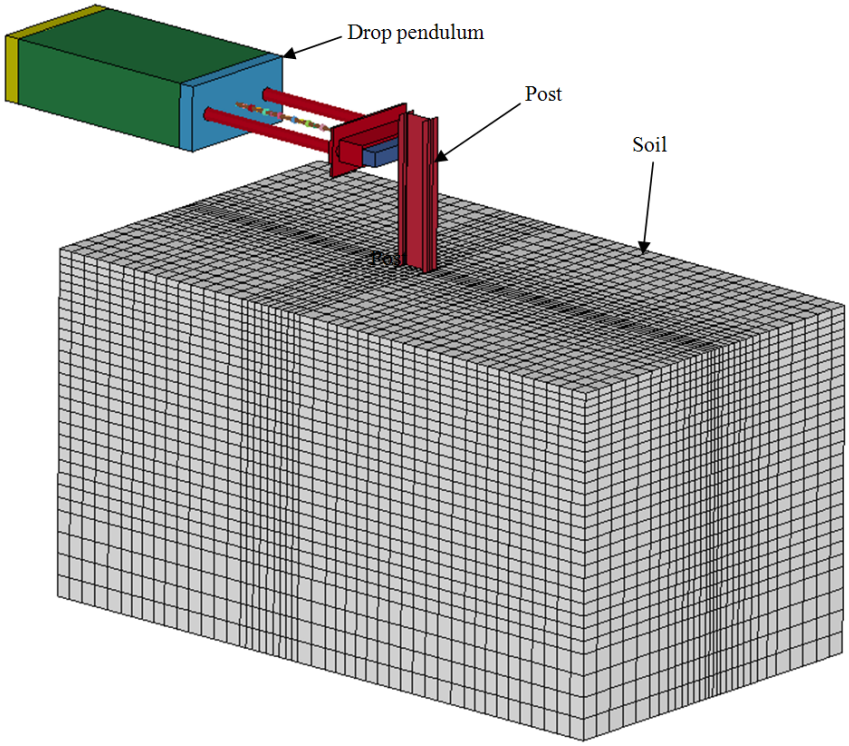

Figure 1: Finite element model of pendulum impacting post in soil.

Using the Geologic Cap model, the researchers were able to calibrate the response of the post and soil model with test results for posts embedded at 1118 mm (44-inch) depth. However, as the embedment depth of the posts decreased, the soil material behavior started to deviate from the response observed in the pendulum tests (see figure 2 for acceleration-time response of the pendulum in simulation and tests). For shallower depths, once the post started to move in the soil, the deceleration remained constant in the simulation results as opposed to a linear deceleration trend observed in the pendulum tests. This was of concern because capturing the post-soil behavior was the basis for developing the guidelines for post installation in rock. The researchers then carried out another extensive exercise of calibrating the Geological Cap model, but the results were not much different.

The researchers then investigated the use of Smooth Particle Hydrodynamics (SPH) technique for modeling the soil. It was argued that as the movement of the post in soil got large, the conventional Lagrangian finite element method may be resulting in an artificially high resistance due to large distortions of the soil mesh. It was expected that a 'meshless' method would eliminate any artificial soil stiffness resulting from the

deterioration of the Lagrangian soil mesh. However, even with the use of SPH modeling, the constant deceleration after the initial deceleration peak was observed. This implied that the problem was less likely to be resulting from the use of a Lagrangian mesh and was more inherent in the Geologic Cap material model. Further use of the SPH modeling technique was therefore discontinued.

The researchers then evaluated other material models available in the LS-DYNA material library for representing the soil. LS-DYNA's Jointed Rock material model (MAT 198) was eventually selected for a new calibration exercise. Several parameters of the soil model were parametrically varied in an extensive calibration exercise. This material model yielded sufficiently reasonable results and the acceleration-time response measured from the simulation matched the response measured in the tests for all embedment depths of the post. Comparisons of acceleration-time responses are presented in figure 3.

W-Beam System Modeling

Having successfully validated the finite element model of the post in soil at various embedment depths, the researchers started developing a finite element model of the standard W-beam guardrail installation with a standard post embedment depth of 1118 mm (44 inches).

The W-beam guardrail system model is shown in figure 4a. The model was comprised of 15 posts spaced at 1905 mm (75 inches). The rail height was 531 mm (21 inches) to the center of the rail. The posts were embedded 1118 mm (44 inches) into the ground. To reduce the size of the model and thus reduce computational cost and time, the end terminals of the W-beam guardrail were not modeled explicitly. Instead, force-deflection response of the end-terminal was incorporated using a non-linear spring element attached to each end of the rail. The spring properties were obtained using a separate model of an end-terminal (see figure 4b). A linearly increasing force was applied to the end-terminal at the rail end that attaches to the W-beam guardrail system. The deflection of the rail was measured for the force applied. This enabled the researchers to develop a force-deflection function of the end-terminal. The force-deflection function was then used to define the stiffness properties of the end-terminal springs used in the W-beam system model (see figure 4c). The use of the spring element in lieu of the explicit end-terminal model resulted in significant savings in computational time without resulting in any significant loss of accuracy.

A 2000 kg (4409 lb) vehicle impacted the W-beam guardrail system with a speed of 100 km/h 62 mi/h) and an angle of 25 degrees as shown in figure 4a. The model was comprised of approximately 430,000 nodes and 380,000 elements. The vehicle model used was developed by the National Crash Analysis Center and included modifications by TTI researchers.

Figure 2: Acceleration-time comparison using Geologic Cap model for various embedment depths.

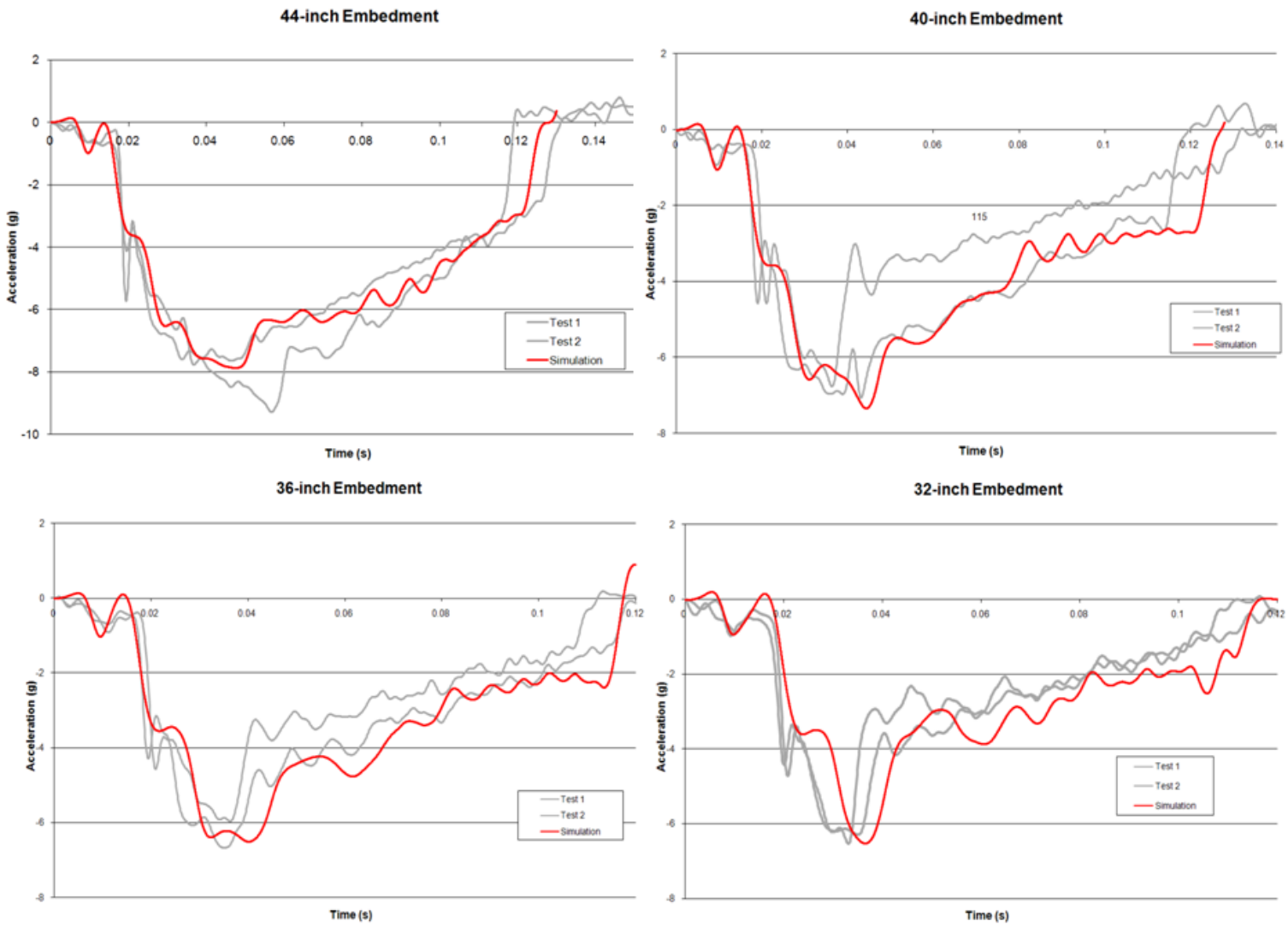

Figure 3: Acceleration-time comparison using Jointed Rock model for various embedment depths.

Results of the W-beam system model simulation were validated using test results of four previously available W-beam guardrail crash tests. In these tests, a 2000 kg (4409 lb) vehicle impacted the W-beam guardrail system at a nominal speed of 100 km/h (62 mi/h) and a nominal angle of 25 degrees. The W-beam guardrail systems in these tests were essentially the same as the one simulated. The main difference between these systems was the type of blockout used. These tests were as follows:

1. 1996, Timber blockouts (405421-1) [*4*]
2. 1997, Recycled polyethylene blockouts (400001-MPT1) [*5*]
3. 2001, Composite blockouts (400001-TRB3) [*6*]
4. 2002, Recycled polymer blockouts (400001-MON1) [*7*]

While different variations of the blockouts were tested, the performance of these blockouts was similar in these tests. Thus, using four crash test results provided a range of W-beam performance for the purpose of validating simulation results.

Figure 5 shows the deformed state of the model after vehicle impact. Table 1 shows a comparison of some of the outcomes of the crash analysis of the W-beam guardrail system. Figure 6 shows a sequential comparison of simulation and test results at approximately 0.24 seconds and 0.48 seconds. As can be seen from the figure, a reasonable correlation in vehicle dynamics exists between simulation and test results. Figure 7 shows comparisons of the vehicle's yaw, pitch, and roll angles. The results obtained from simulation analysis adequately correlate to the range of results obtained from the crash testing. The W-beam system model was thus considered sufficiently valid and was used further in the parametric analyses.

Parametric Analysis with Posts at Reduced Embedment

The objective of these parametric analyses was to perform *NCHRP Report 350*, Test Level 3 simulations with the W-beam guardrail system when one or more posts were 'compromised.' A post was considered 'compromised' if it was installed at an embedment depth of less than 1118 mm (44 inches), or was missing all together. This was considered equivalent to the case when a post is not installed with proper embedment depth due to the presence of rock. The results of simulations with several combinations of compromised posts were to be used to develop preliminary guidelines for installation of guardrail posts in rock.

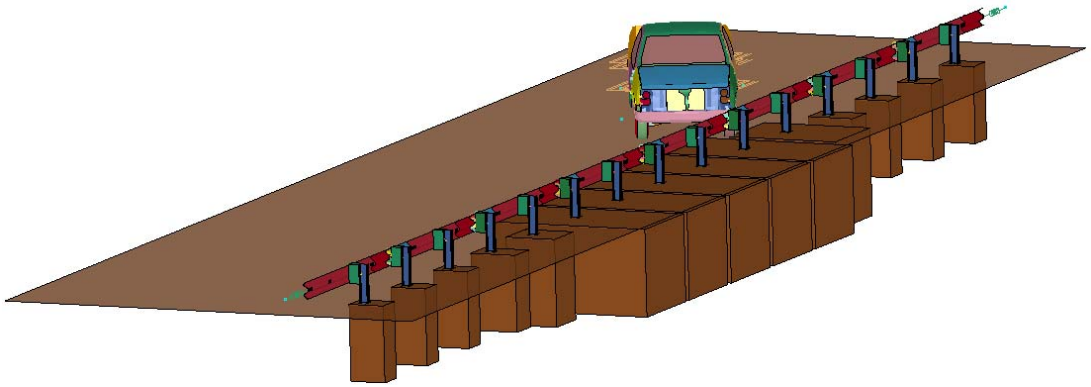

(a) System model

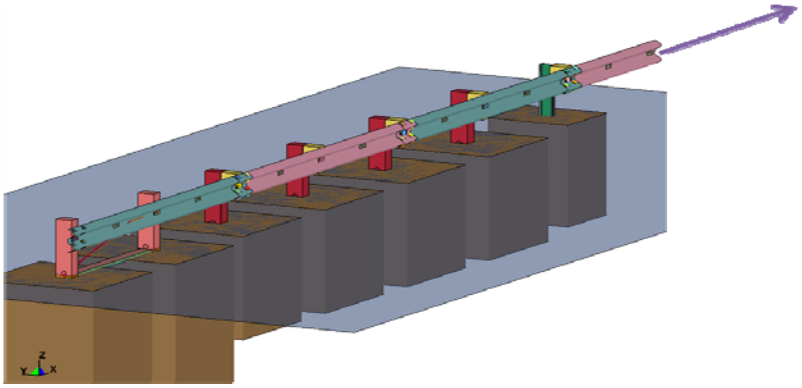

(b) End-terminal model

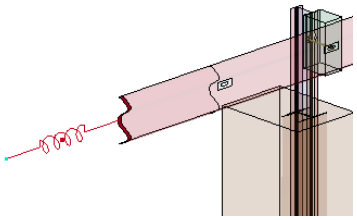

(c) End-terminal spring

Figure 4: W-beam guardrail system model.

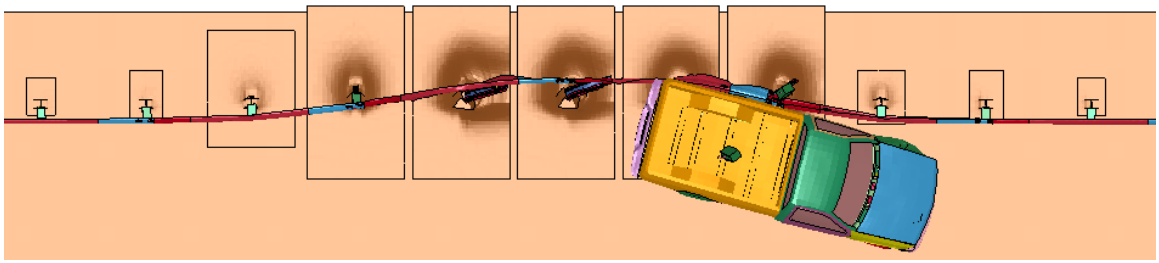

Figure 5: Results of the W-beam guardrail simulation.

Table 1: Comparison of several post-impact parameters

	Simulation	405421-1	400001MPT1	400001TRB3	400001MON1
Max. dynamic deflection (m)	1.1	1	1.3	0.89	0.837
Total contact length (m)	8.4	5.8	10.3	8.13	unknown
Number of posts where rail detached	4	3	5	2	3
Vehicle exit speed (km/h)	46.4	55	46.12	59.4	49.4

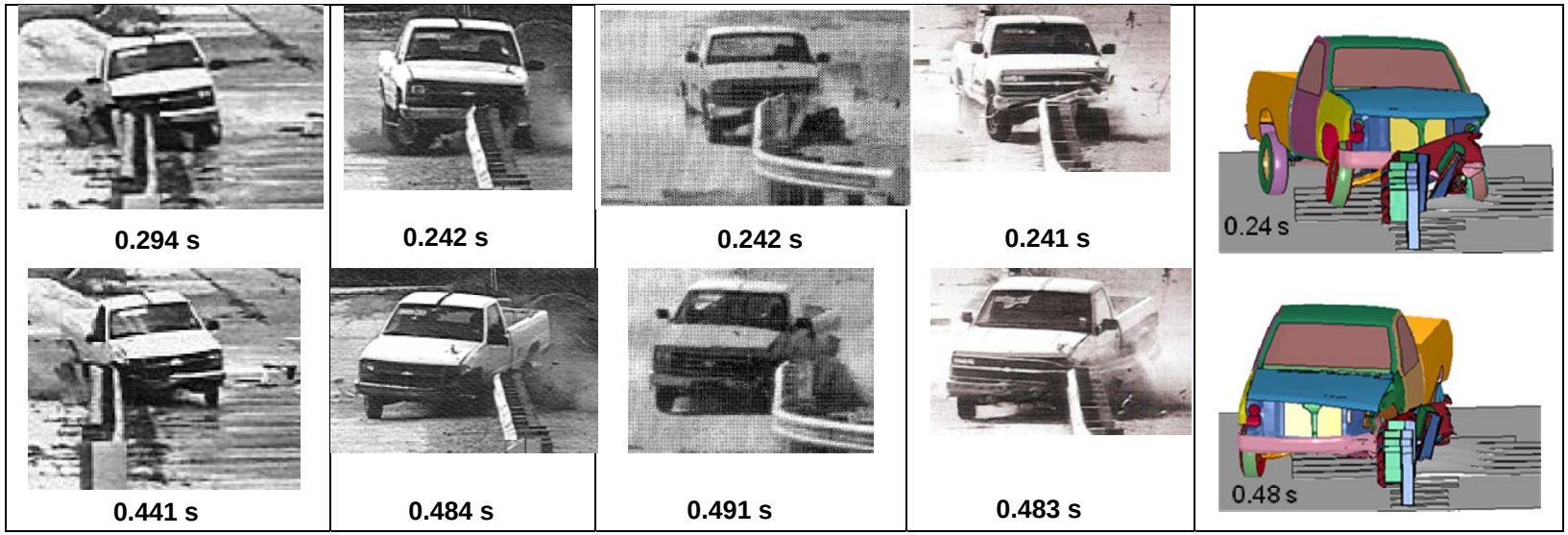

Figure 6: Comparison between simulation and the four tests at nearly same points in time.

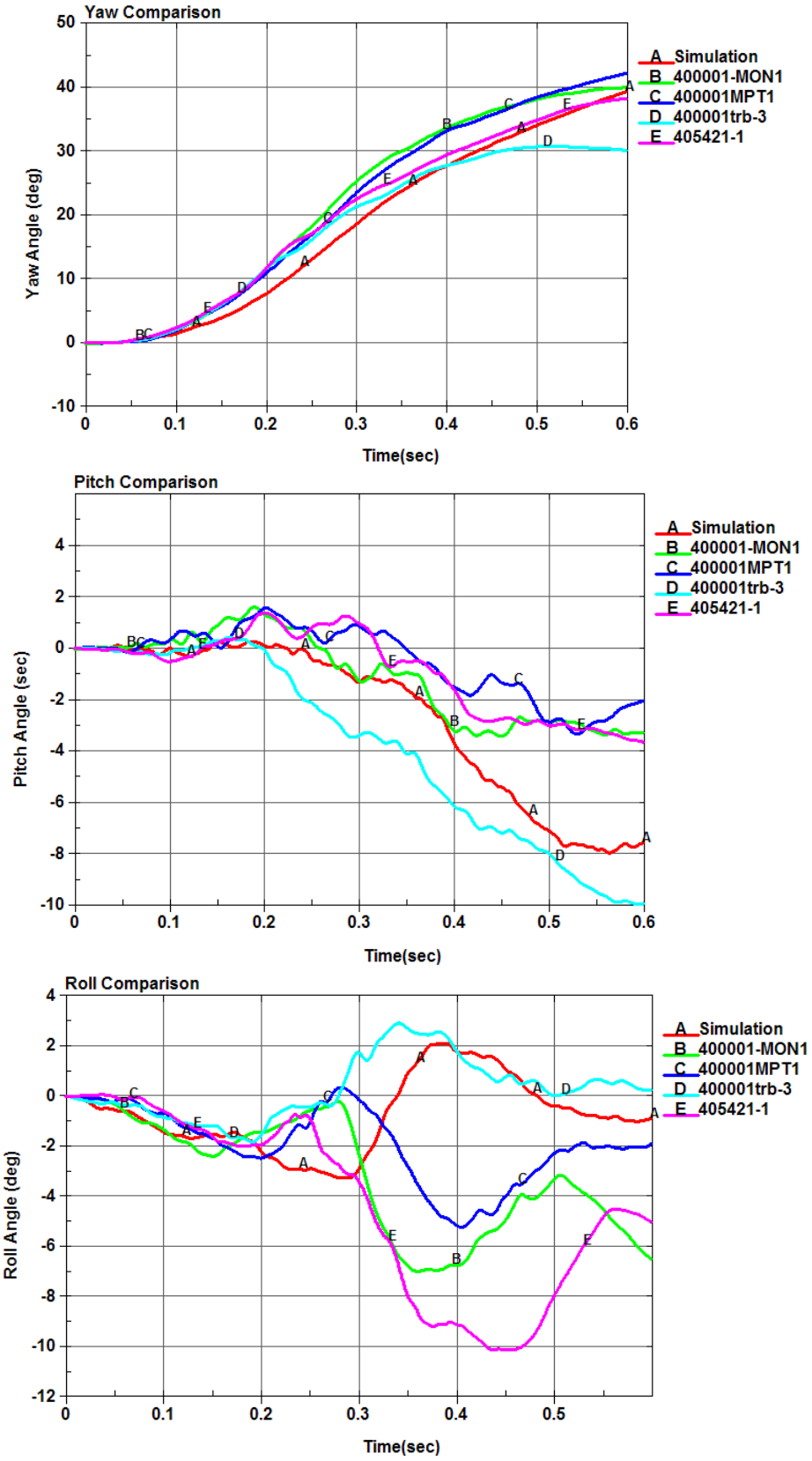

Figure 7: Comparison of vehicle's yaw, pitch, and roll angles.

As a first step, the researchers performed a simulation with one of the posts missing from the W-beam guardrail installation. This would be equivalent to the case when rock is encountered at the ground surface and thus the post is left out to avoid drilling in the rock. The 2000 kg (4409 lb) vehicle impacted the barrier at a speed of 100 km/h (62 mi/h) at an angle of 25 degrees. Simulation results indicated that the vehicle was redirected successfully and no signs of vehicle pocketing or overriding were observed. The researchers then performed another simulation with two consecutive posts removed from the W-beam guardrail system. Simulation results indicated that the vehicle redirected without any significant concerns of pocketing or overriding in this case as well. To judge the sensitivity of the model to missing posts, the researchers performed another simulation with three consecutive posts missing. The results were not much different from the previous two cases and the vehicle redirected successfully. The deformed states of the W-beam guardrail are shown in figure 8 for the three cases described. The successful redirection of the vehicle with up to three posts missing, without a significant deterioration in guardrail performance, raised doubts regarding the sensitivity of the model and its ability to accurately predict the guardrail performance.

Prior testing has shown that longer unsupported spans of W-beam guardrail require special design modifications for acceptable guardrail performance. In 2007, MwRSF developed the Midwest Guardrail System (MGS) in which three consecutive posts were removed [*8*]. The system was successfully crash tested to meet *NCHRP Report 350* TL-3 requirements. Features of this system that differed from conventional strong post W-beam guardrail included using special breakaway wood posts at each end of the long span, using deeper blockouts, raising rail height, and moving the rail splices away from the posts. The use of deeper blockouts helps in reducing wheel snagging. The use of breakaway wood posts helps in eliminating any vehicle pocketing that develops during redirection. Offsetting the splices away from the posts helps prevent high stress concentration in the splice area where rail segments overlap, thus decreasing chances of rail rupture at a splice. The modifications made to the standard W-beam guardrail design were therefore essential in successful performance of the W-beam system for longer spans. In 2006, TTI performed a crash test of a nested long-span W-beam guardrail [*9*]. Two of the posts were missing in the system, thus making a long span of 5.7 m (18 ft – 9 inches). Nested W-beam rail (two layers) was installed over a length of 11.4 m (37 ft – 6 inches), which covered the long span, one upstream span, and two downstream spans. As the vehicle was redirecting in the crash test, the guardrail rail ruptured at the splice where the nested rail transitioned to the single W-beam rail, resulting in a failed test.

Thus, based on previous crash testing experience with long-span W-beam guardrail systems, it was concluded that longer spans of W-beam guardrail with two or more posts missing require special design changes for successful guardrail performance. Even though the results of simulations performed with one, two, and three posts missing showed some of the expected differences, such as increased lateral rail deflection, the results were not significantly different. In other words, the results of the simulations for these cases were not discerning enough to make a “pass” or “fail” judgment on the performance of the guardrail systems.

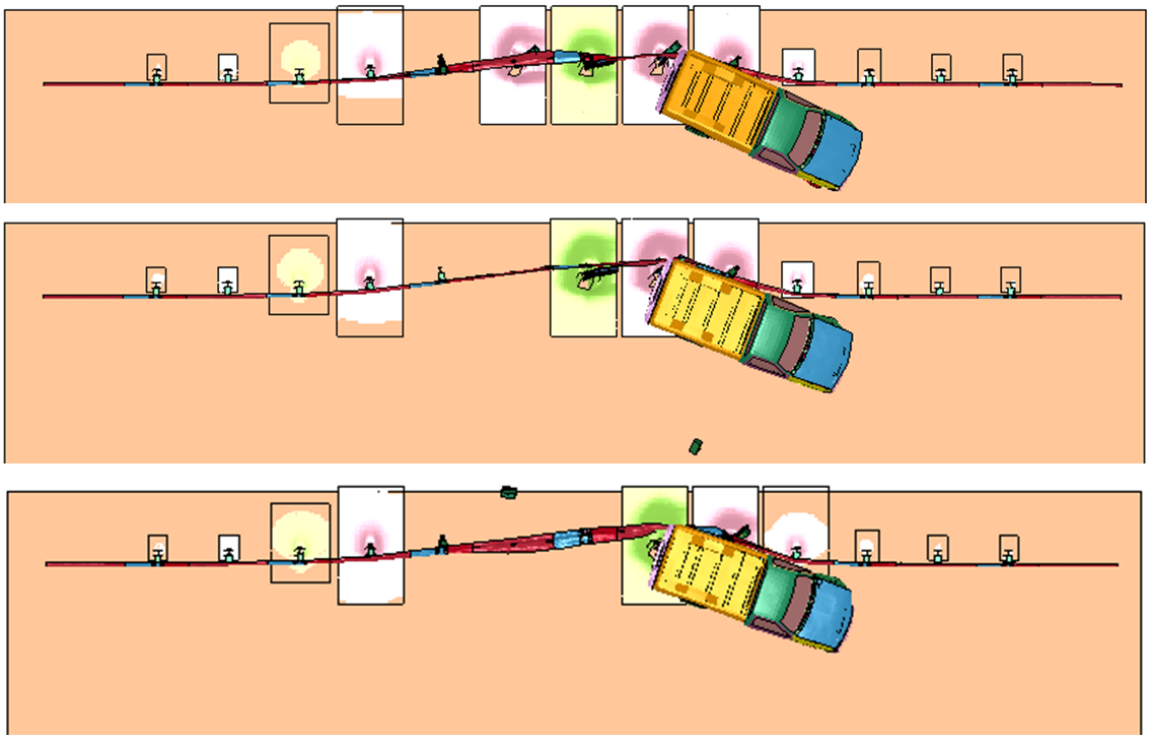

Figure 8: Deformed state of the W-beam as the vehicle exits the system. Top: One post missing, Middle: Two posts missing, Bottom: Three posts missing.

The researchers evaluated several other aspects of the W-beam guardrail system model with the objective of improving its sensitivity in evaluating guardrail performance with compromised posts. The effect of the Critical Impact Point (CIP) on the performance of W-beam guardrail systems with compromised posts was investigated in greater detail. The CIP was calculated based on the average post spacing and post depths in the region of impact and the simulations with the missing posts were repeated. The results of the simulations however did not show significant differences with variations in CIP.

The researchers also looked at the effect of variation in material properties of the W-beam guardrail on the overall performance of the system. The initial guardrail model incorporated the rail material properties determined by Reid et al. [*10*]. The yield stress of the material was determined to be 450 MPa (65 ksi). Recent testing of guardrail steel conducted under a separate project during the course of this research revealed a much lower yield of 386 MPa (56 ksi), which also meets the AASHTO M 180 specification for W-beam guardrail material (i.e. minimum yield of 345 MPa (50 ksi). The researchers repeated the simulations with one, two, and three posts missing using the weaker W-beam guardrail material properties. While some differences were observed in the results, the results did not show a significant increase in vehicle pocketing, or the potential for the vehicle to override the barrier.

The researchers also performed simulations for cases when all posts were present, but some were installed at a reduced embedment depth. Simulations were performed with two and three consecutive posts installed at a reduced embedment depth of 813 mm

(32 inches). As before, while some differences existed between the results, the differences were not discerning enough to indicate that any of the configurations would have unacceptable impact performance.

In addition to the modes of failure where a vehicle starts pocketing into the guardrail or starts to override the rail, the researchers looked at the potential for rail rupture during impact. The rupture of rail during vehicle impact is a relatively complex phenomenon. The rail usually ruptures as a result of a small tear that is initiated due to a sharp contact with the flange of the deflecting post, the edge of the blockout, an exposed edge of the damaged vehicle, etc. Traditional finite element analysis techniques lack a validated and robust material failure capability for the guardrail; therefore the ability to evaluate rail rupture was limited. Contours of plastic strains in the W-beam guardrail were compared for the simulated cases. The objective of the comparison was to identify areas of high strain that may indicate a potential for material failure, thus causing the rail to rupture. For each simulation of the W-beam system with compromised posts, the contours of plastic strains were compared to the contours observed in the standard W-beam guardrail simulation. However, this comparison did not show a reliable pattern of increasing high strain areas with increasing number of compromised posts. The comparison could therefore not be used to decide with enough confidence whether certain configurations of compromised posts would fail due to guardrail rupture.

More recently, failure of thin sheet metal (such as the W-beam guardrail) is being incorporated in finite element simulations in the automotive industry. However this requires determining several material properties of the steel for the Gurson material model in LS-DYNA (or other similar material models) as opposed to the piecewise-linear-plasticity material model traditionally used for modeling steel [*11*]. It also requires a validation of the ability and robustness of the model to capture material failure by performing small scale rail rupture tests and replicating the results using the new material model. Development of a material failure model using this advanced method was not within the scope of this research and was therefore not attempted. However, the researchers note that such work could be considered in future research involving failure of thin metal components such as the W-beam guardrail.

Summary and Conclusions

The objective of this research was to develop preliminary guidance for the installation of W-beam guardrail posts when encountered by the presence of rock. The work was proposed to be completed in two phases. In the first phase, reported herein, the researchers were to use simulation analysis to evaluate the performance of the W-beam guardrail under different scenarios where one or more posts were either missing or installed at a reduced embedment due to the presence of rock. The simulation analysis was to be used to determine if a particular configuration would "pass" or "fail" under *NCHRP Report 350* testing criteria and thus develop preliminary guidelines for guardrail post installation when rock is encountered. If the members of the pooled fund states were to find the preliminary guidelines acceptable, a second phase would be funded in which

crash testing would be performed to verify the preliminary guidelines and develop final guidelines.

To develop the preliminary guidelines through finite element simulation analysis, the researchers conducted a series of pendulum tests involving W-beam guardrail posts installed in soil at reduced embedment depths. The researchers then developed the finite element models for these post and soil configurations. An extensive calibration exercise was performed to determine an appropriate soil material model and properties that would enable the post-soil behavior of the model to match the behavior observed in the tests for different embedment depths.

Once the post-soil response was successfully captured, the researchers developed a full-scale model of a standard strong post W-beam guardrail system and performed a successful validation of the model using data from previously conducted crash tests.

After validation of the standard W-beam guardrail model, a parametric evaluation of W-beam guardrail performance was performed. In this evaluation, several cases were simulated with one or more posts either missing from the system or installed at reduced embedment depth due to the presence of rock or other below grade obstruction. At this stage, it was determined that the W-beam guardrail model did not exhibit certain modes of failure (such as vehicle pocketing, rail rideover, etc) that would be expected under certain extreme cases (such as when three posts are missing). While the simulation results showed certain trends that suggested improvement or worsening of W-beam performance, the results were not discerning enough to make the "pass" or "fail" judgment needed to develop the preliminary guidelines for post installation in rock. Several modifications and improvements were made to the model to improve its sensitivity in predicting guardrail performance with compromised posts. While some improvements were made in the sensitivity of the model, the issue was not resolved.

Currently used modeling and simulation techniques in the roadside safety community for modeling the W-beam guardrail system are not able to exhibit some of the failure modes necessary for developing the preliminary guidelines. While some new methods such as using alternate material models for incorporating rail rupture could be explored, more resources were needed and it could not be guaranteed that the desired sensitivity of the model would be achieved.

An alternate method of developing the guidelines is through a program of full-scale crash testing. However, this method would require a funding level that currently exceeds the financial capacity of the pooled-fund. It is, therefore, recommended that a problem statement be developed for a national level research project under NCHRP. This would provide the level of funding needed to develop the guidelines for post installation in rock through a program of full-scale crash testing.

References

[1] Hirsch T.J. and Beggs D. (1987). “Use of Guardrails on Low Fill Bridge Length Culverts.” Research Report 405-2F, Texas Transportation Institute, Texas.

[2] Herr J.E., Rohde J.R., Sicking D.L., Reid J.D., Faller R.K., Holloway J.C., Coon B.A. and Polivka K.A. (2003). “Development of Standards for Placement of Steel Guardrail Posts in Rock.” Research Report TRP-03-119-03, Midwest Roadside Safety Facility, Nebraska.

[3] Baxter, J. R. (2004). “W-Beam Guardrail Installations in Rock and in Mowing Strips.” Memorandum HAS-10/B64-B, Federal Highway Administration, U.S. Department of Transportation, Washington D.C.

[4] Bullard D.L., Menges W.L. and Alberson D.C. (1996). “NCHRP report 350 Compliance Test 3–11 of the Modified G4(1S) Guardrail with Timber Blockouts.” Report FHWA-RD-96-175, Texas Transportation Institute, Texas.

[5] Bligh, R.P., and Menges, W.L. (1997). “Testing and Evaluation of a Modified Steel Post W-Beam Guardrail System with Recycled Polyethylene Blockouts.” Report 400001-MPT, Texas Transportation Institute, Texas.

[6] Alberson D.C. Menges W.L. and Schoeneman S.K. (2001). “NCHRP Report 350 Test 3-11 of the Strong Post W-beam Guardrail with Trinity Composite Blockout.” Contract P20001281, Texas Transportation Institute, Texas.

[7] Williams W.F., Menges W.L. and Haug R.R. (2002). “NCHRP Report 350 Test 3-11 of the G-4 W-beam Guardrail with Mondo Recycled Polymer Offset Block.” Report 400001-MON1, Texas Transportation Institute, Texas.

[8] Bielenberg, R.W., Faller, R.K., Rohde, J.R., Reid, J.D., Sicking, D.L., Holloway, J.C., Allison, E.M., and Polivka, K.A., (2007). "Midwest Guardrail System for Long-Span Culvert Applications." Transportation Research Report No. TRP-03-187-07, Midwest Roadside Safety Facility, University of Nebraska-Lincoln, Nebraska.

[9] Buth C.E., Bullar D.L and Menges W.L. (2006). “NCHRP Report 350 Test 3-11 of the Long-span Guardrail with 5.7 m Clear Span and Nested W-beams Over 11.4 m.” Report 405160-1-1, Texas Transportation Institute, Texas.

[10] Reid J. D., Bielenberg B. W. (1999). “Using LS-DYNA Simulation To Solve a Design Problem: Bullnose Guardrail Example.” Transportation Research Record No. 1690, Transportation Research Board, Washington D.C.

[11] Livermore Software Technology Corporation. (2007). “LS-DYNA Keyword User’s Manual.” Livermore Software Technology Corporation, California.

Geometric Optimization of Existing Guidelines for W-Beam Guardrail Post Installation in Rock

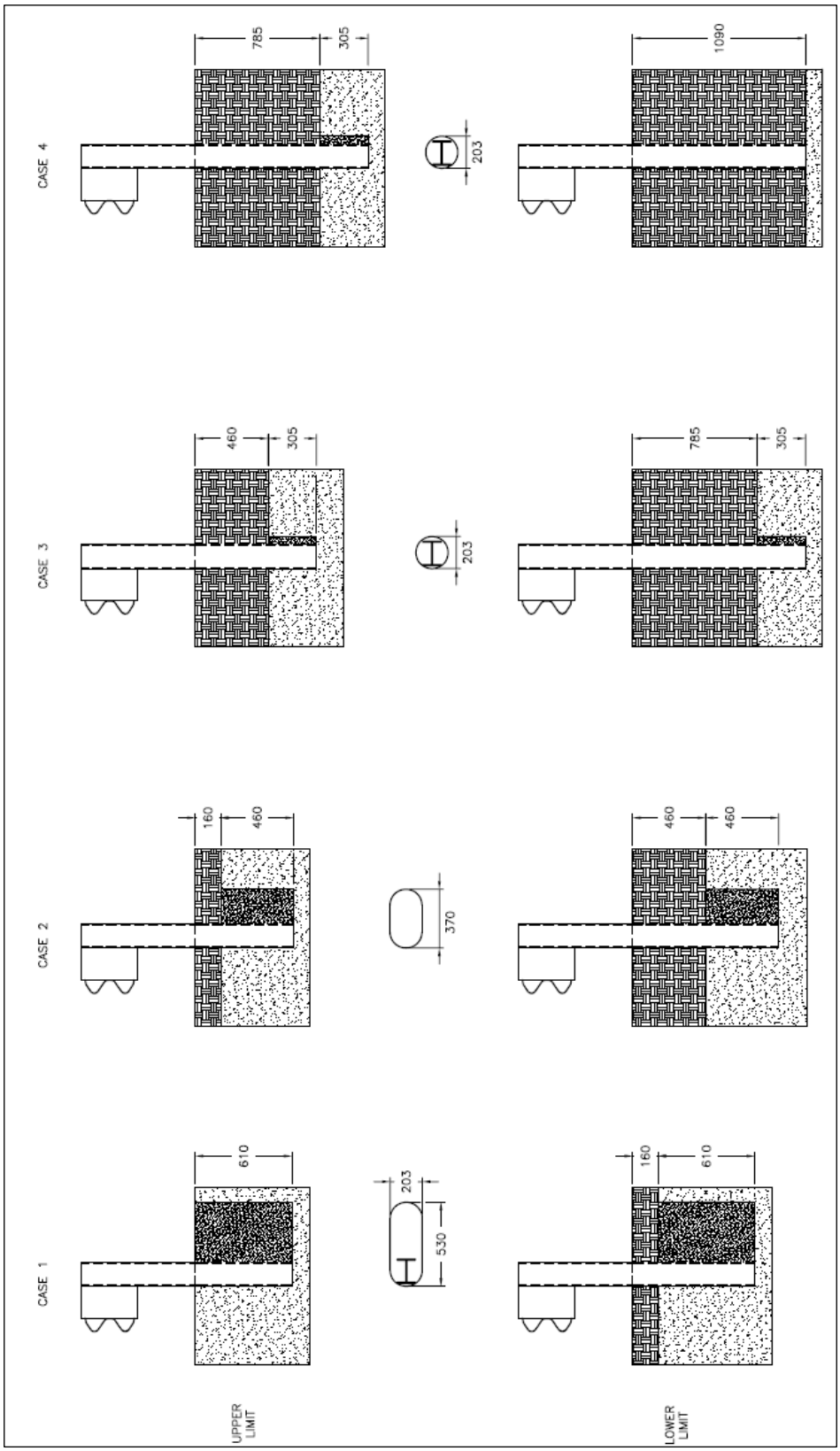

Figure A-1: MwRSF's detailed guideline for post installation in rock (dimensions in mm).

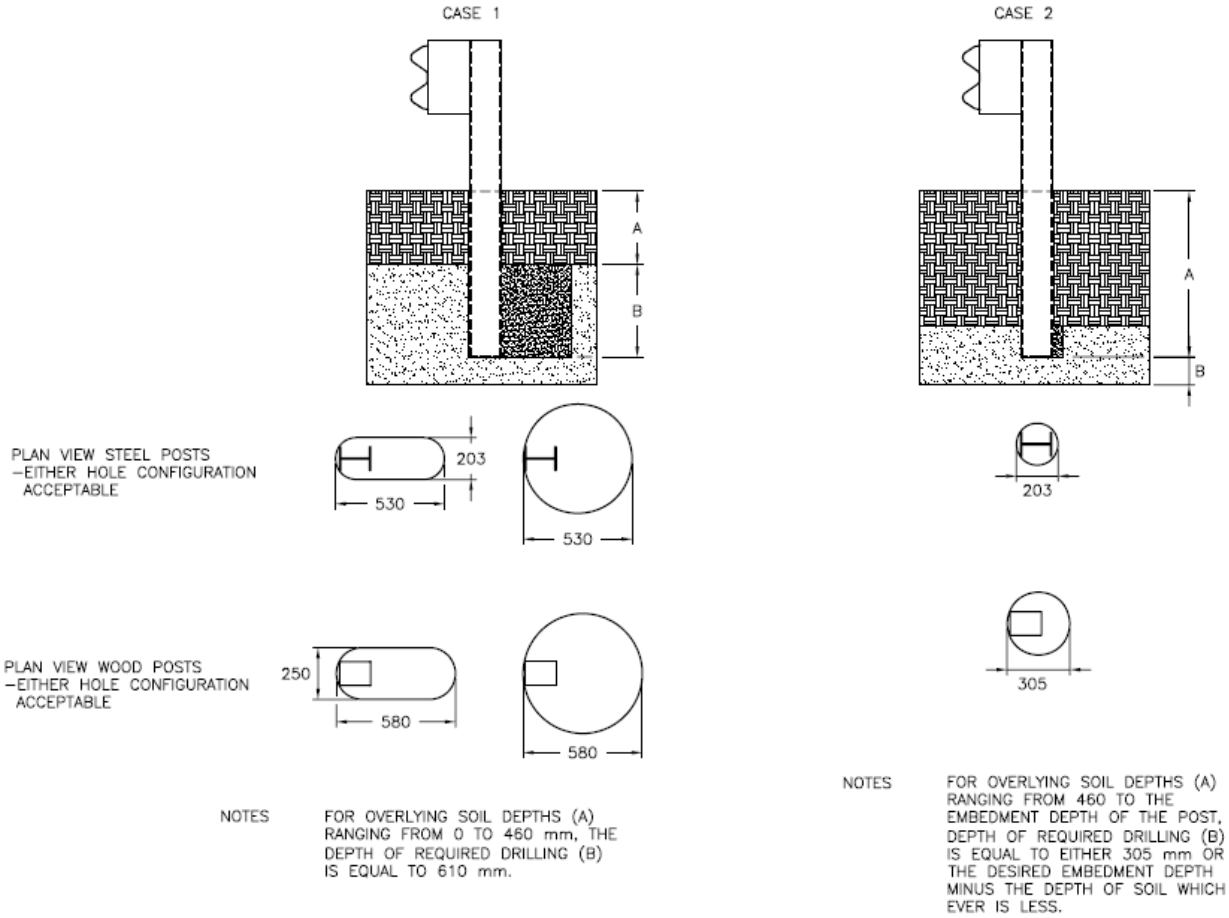

Figure A-2: Coring requirements specified in FHWA's memorandum (dimensions in mm).

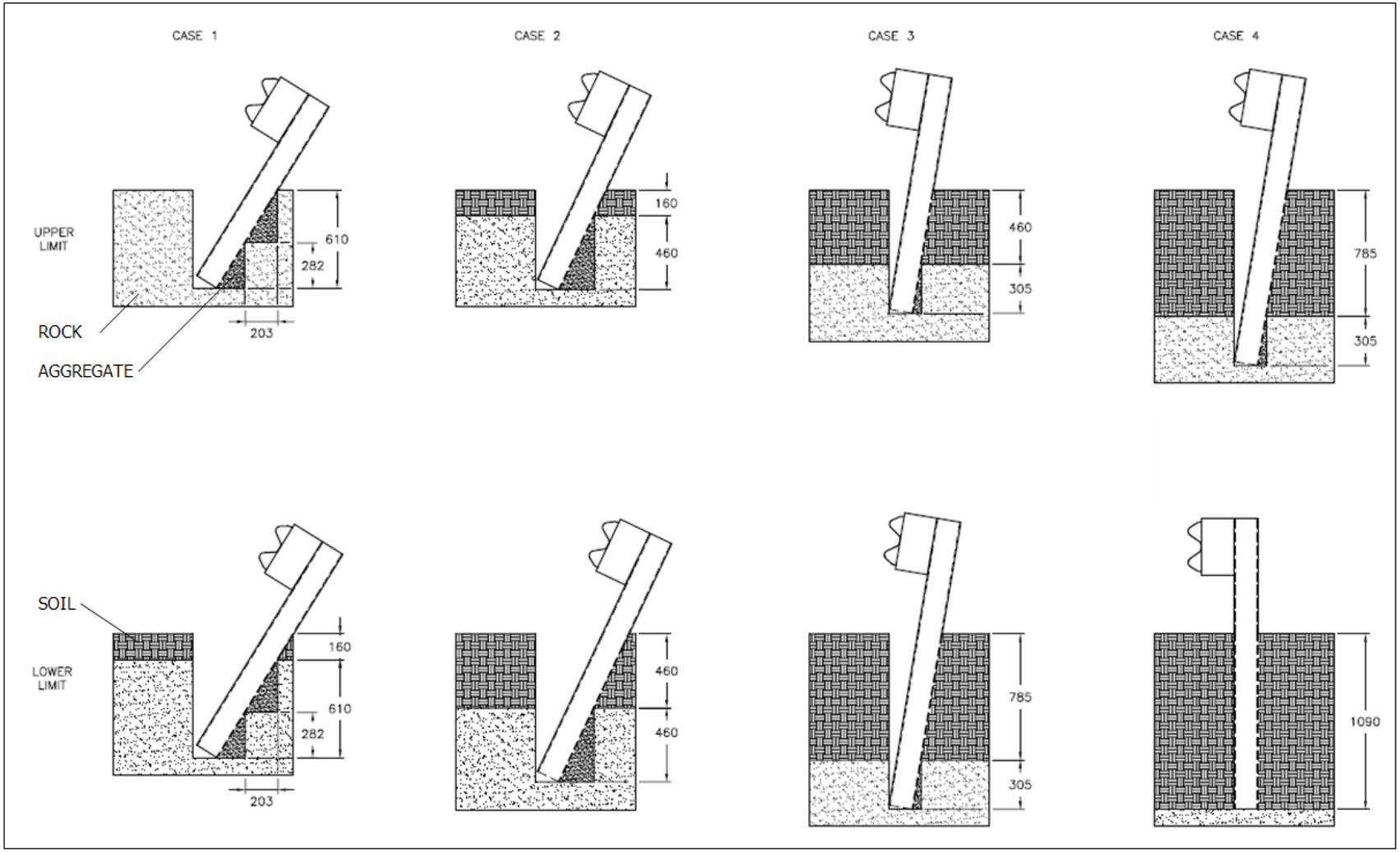

Figure A-3: TTI's evaluation of the existing guidelines through geometric optimization (dimensions in mm).

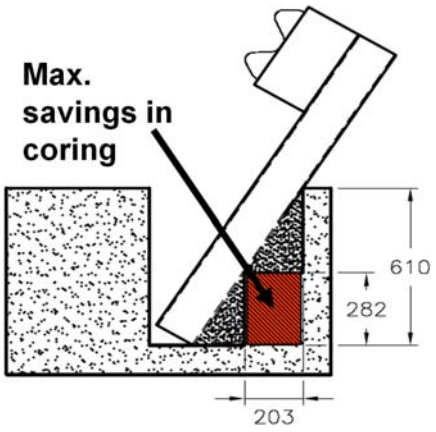

Figure A-4: A small reduction in rock drilling can be attained are for Case 1 (dimensions in mm).

ATTACHMENT-B

Pendulum Testing of W-Beam Guardrail Posts Installed in Soil at Various Embedment Depths

To evaluate the performance of the W-beam guardrail posts embedded at various depths in soil, the researchers performed several pendulum impact tests. In these tests, an 839 kg (1850-lb) drop pendulum with a crushable nose impacted the embedded posts at a speed of 35 km/h (22 mph). The acceleration-time response measured from on the pendulum's body was used to determine the overall response of the embedded posts.

The embedded posts were tested at Texas Transportation Institute's (TTI) outdoor pendulum testing facility. The pendulum bogie was built according to the specifications of the Federal Outdoor Impact Laboratory's (FOIL) pendulum. The testing area is shown in figure B 1. Frontal crush of the aluminum honeycomb nose of the bogie simulates the crush of an actual vehicle. A sweeper plate constructed of steel angles and a steel plate is attached to the body of the pendulum with a ground clearance of 152 mm (6 inches) to replicate an automobile's undercarriage. The crushable nose configuration of the pendulum is similar to the FOIL ten-stage bogie nose. Cartridges of expendable aluminum honeycomb material of differing densities are placed in a sliding nose assembly. The pendulum impacts the post at a target speed of 35 km/h (22 mph) and at a height of 460 mm (18 inches) above the ground, which represents the bumper height of a small passenger car. After each test, the honeycomb material is replaced and the pendulum is reused. A sketch of the honeycomb nose configuration used for the pendulum bogie is shown in figure B 2. Testing was performed in accordance with *NCHRP Report 350* procedures.

Figure B-1: Texas Transportation Institute Proving Ground's outdoor pendulum facility.

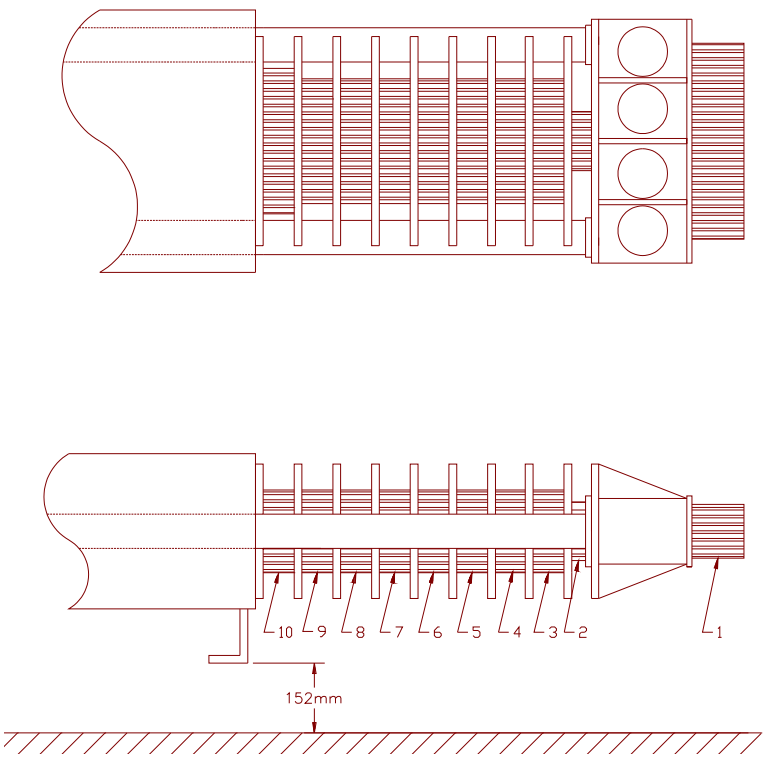

Cartridge Number	Size (mm)	Area Effectively Removed by Pre-Crushing (mm^2)	Static Crush Strength (kPa)	Total Crush Force for Each Cartridge (kN)
1	69.9 × 406 × 76		896.3	25.4
2	102 × 127 × 51		172.4	2.2
3	203 × 203 × 76	13549	896.3	24.8
4	203 × 203 × 76	9678	1585.8	50.0
5	203 × 203 × 76	3871	1585.8	59.2
6	203 × 203 × 76		1585.8	65.3
7	203 × 203 × 76	13549	2757.9	76.3
8	203 × 203 × 76	7742	2757.9	92.3
9	203 × 203 × 76		2757.9	113.6
10	203 × 254 × 76		2757.9	142.3

Figure B-2: Configuration of the pendulum nose and the honeycomb cartridges.

A total of 12 pendulum tests were performed on W152×13.4 (W6×8.5) steel and 152 × 203 mm (6×8-inch) wood posts at various embedment depths as shown in table B-1. The tests were performed on two different days and in the order presented in table B-1. Figure B-3 shows a typical test article setup prior to impact.

Table B-1: Test Matrix for Pendulum Testing

Test Day 1		
Test No.	**Post Type**	**Depth (in.)**
P1	W6x8.5 Steel	44
P2	W6x8.5 Steel	40
P3	W6x8.5 Steel	36
P4	6 in. x 8 in. Wood	44
P5	W6x8.5 Steel	32
Test Day 2		
Test No.	**Post Type**	**Depth (in.)**
P6	W6x8.5 Steel	44
P7	6 in. x 8 in. Wood	44
P8	W6x8.5 Steel	40
P9	W6x8.5 Steel	36
P10	6 in. x 8 in. Wood	36
P11	W6x8.5 Steel	24
P12	W6x8.5 Steel	32

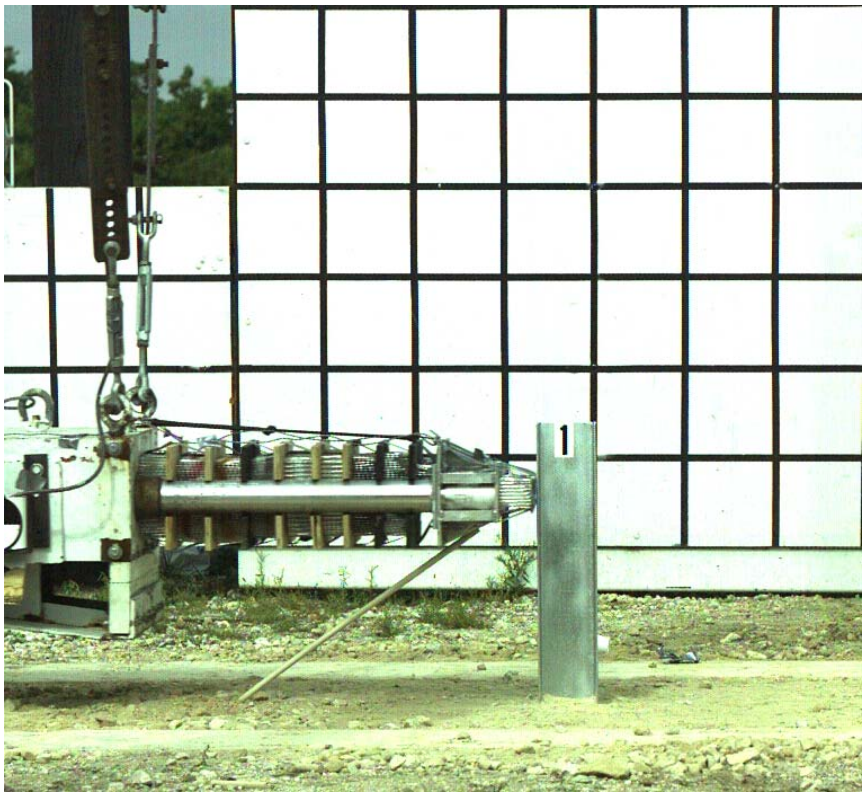

Figure B-3: Typical test setup.

With the exception of test P6, none of the steel posts were deformed after the pendulum impact. In test P6, slight bending of the post was observed at ground level, which resulted in a permanent deflection of 102 mm (4 inches) about the strong axis and 95 mm (3.75 inches) about the weak axis at the top of the post. None of the wood posts fractured in the tests. The acceleration-time responses of the tests are presented in Figures B-4 through B-15.

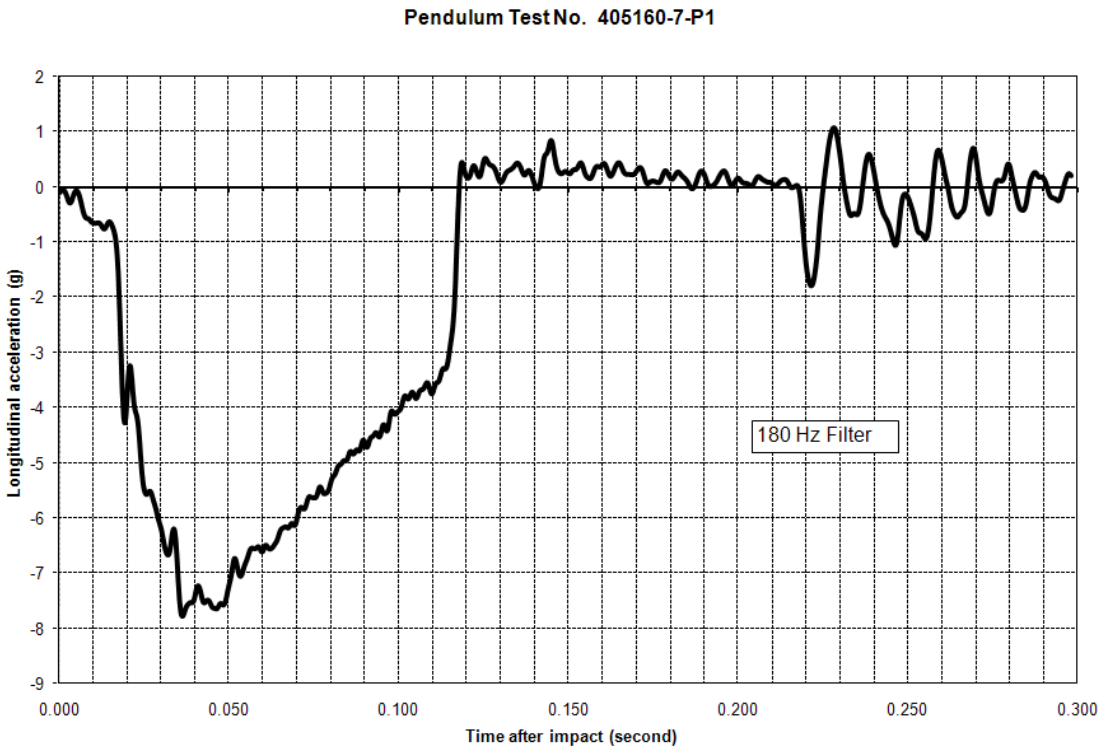

Figure B-4: Acceleration-time response from test P1.

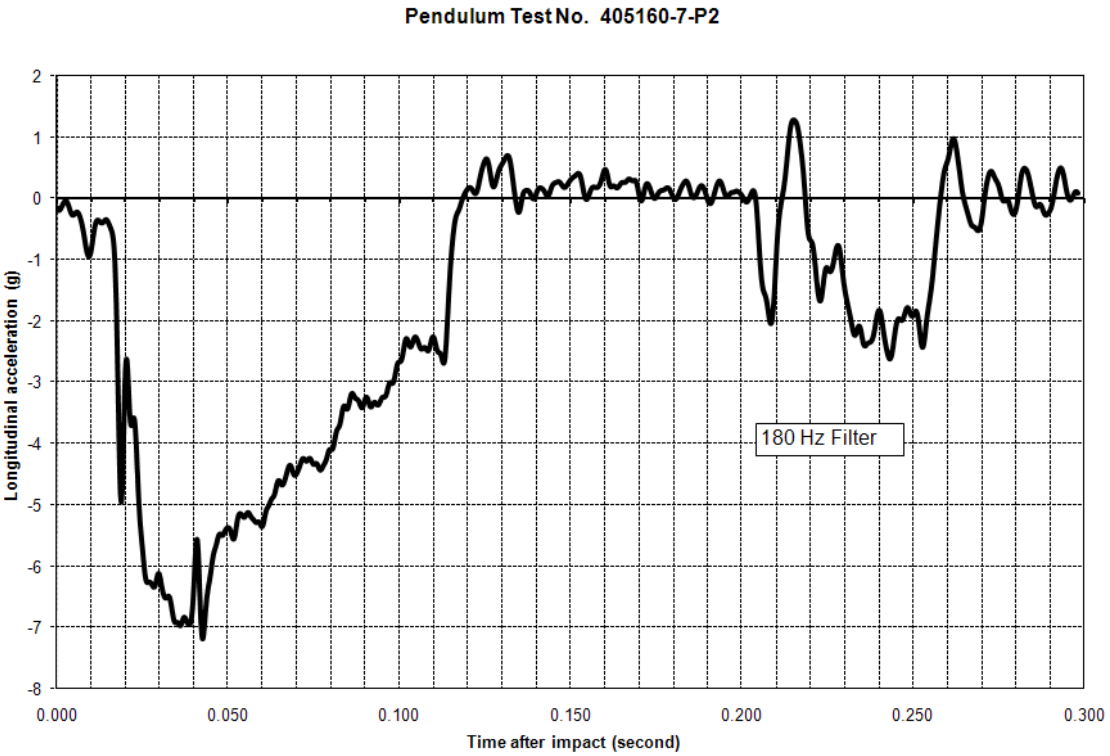

Figure B-5: Acceleration-time response from test P2.

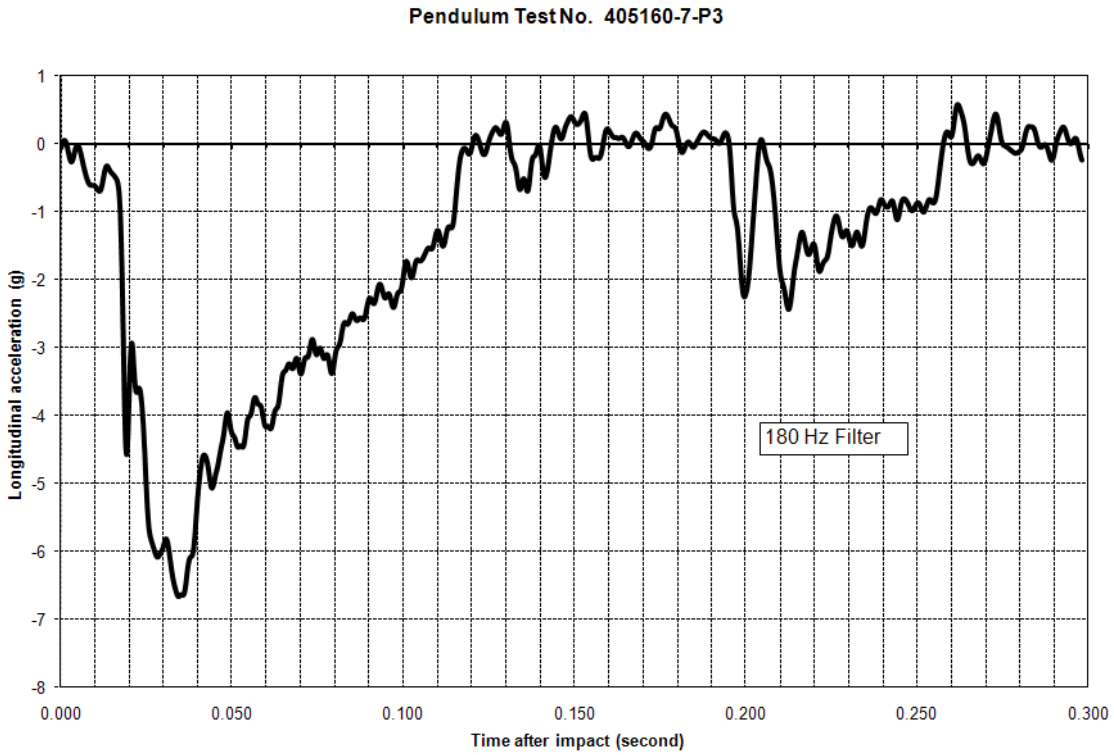

Figure B-6: Acceleration-time response from test P3.

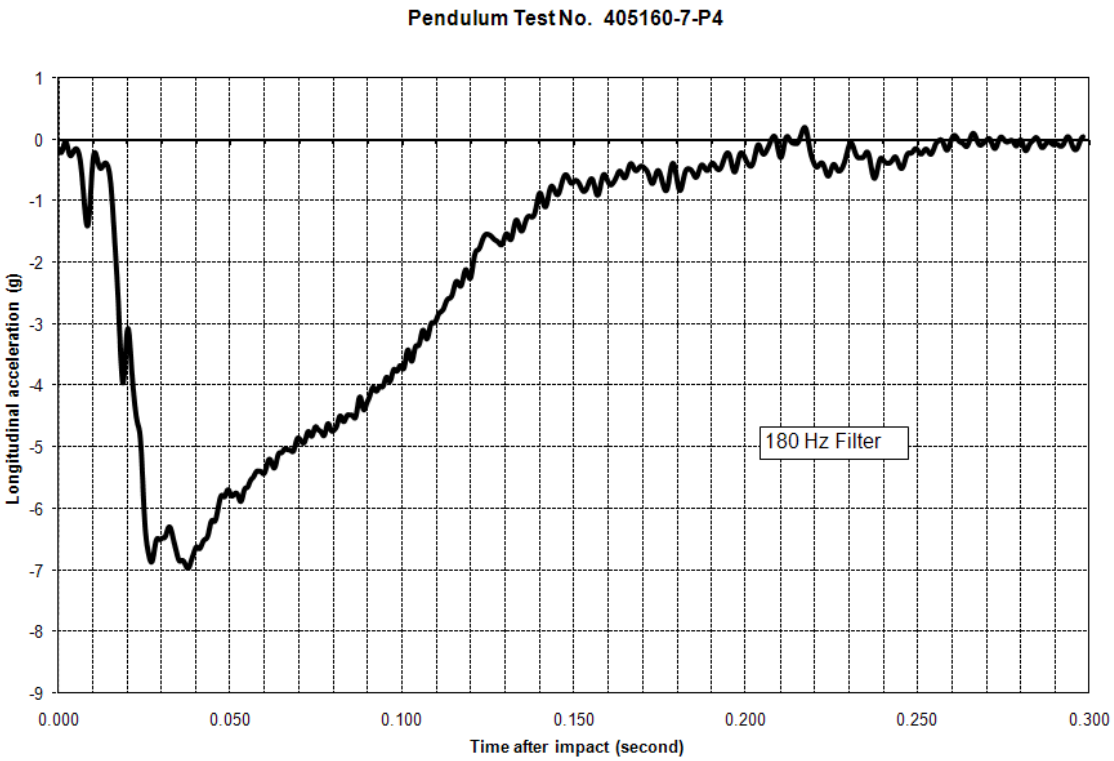

Figure B-7: Acceleration-time response from test P4.

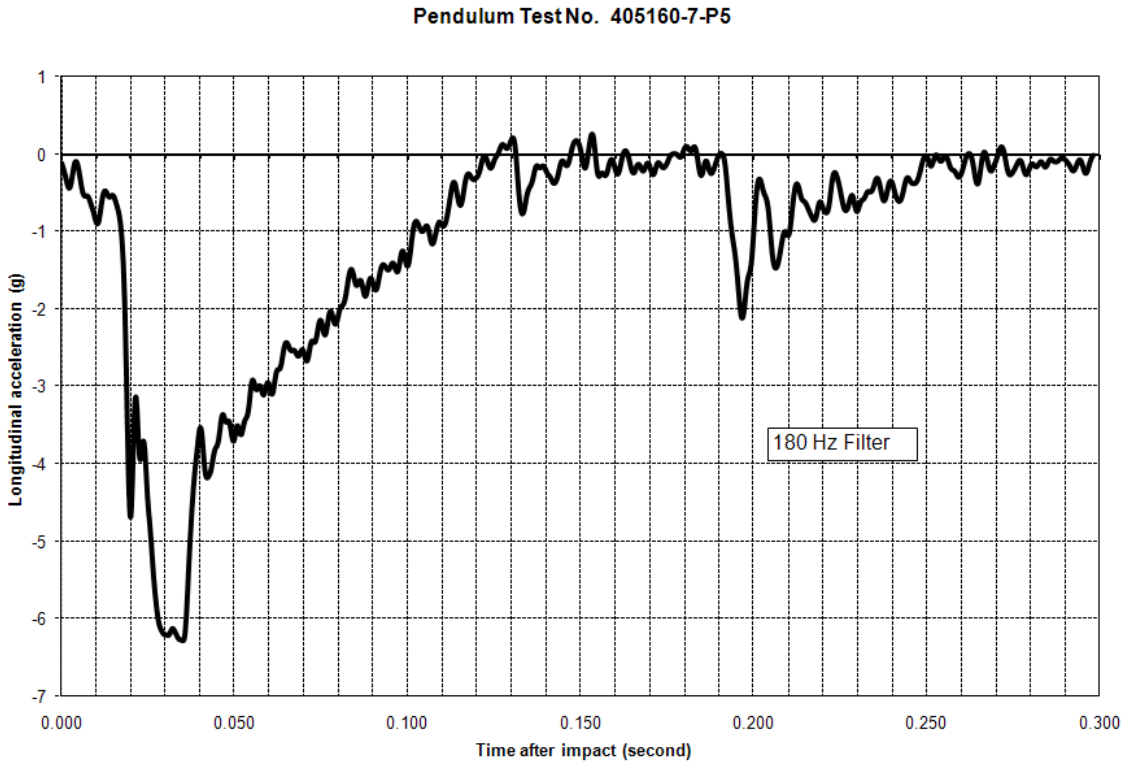

Figure B-8: Acceleration-time response from test P5.

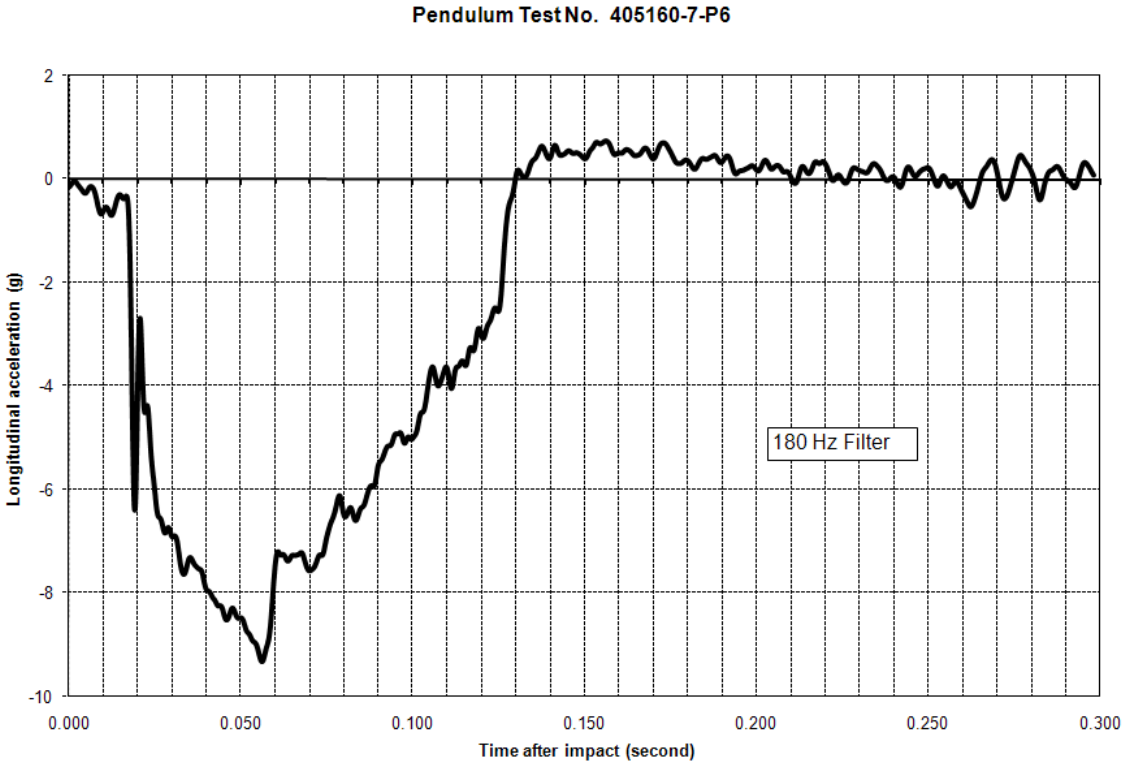

Figure B-9: Acceleration-time response from test P6.

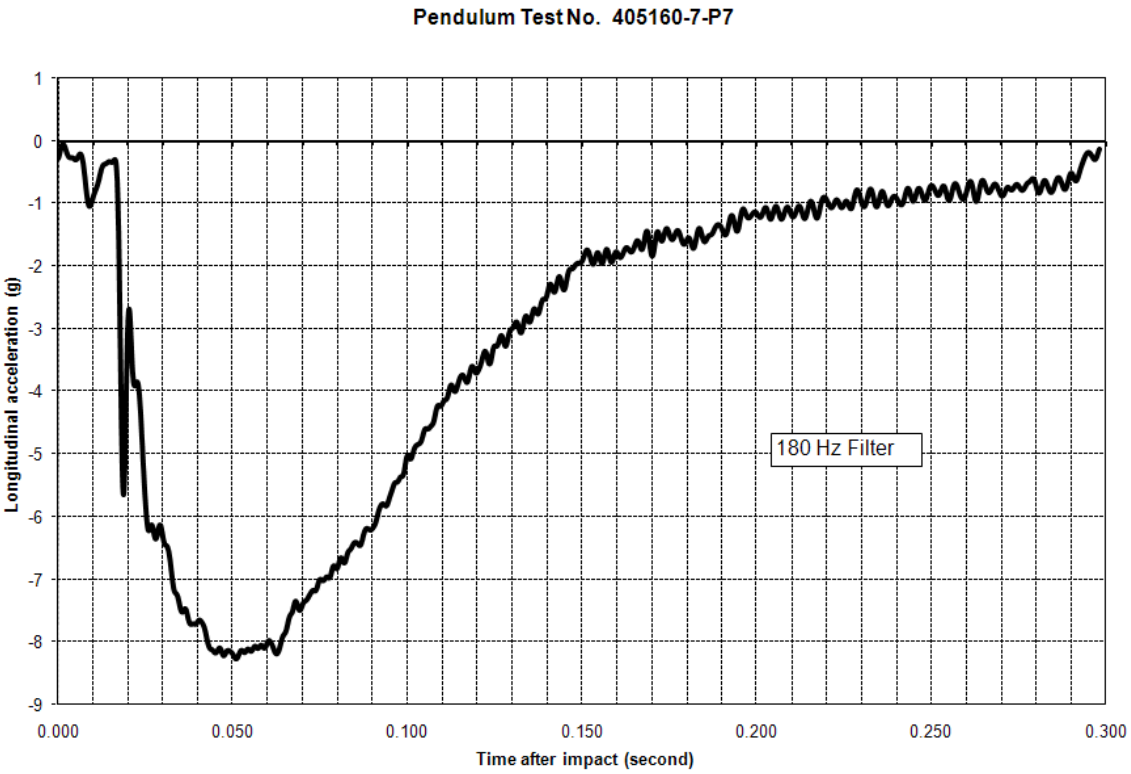

Figure B-10: Acceleration-time response from test P7.

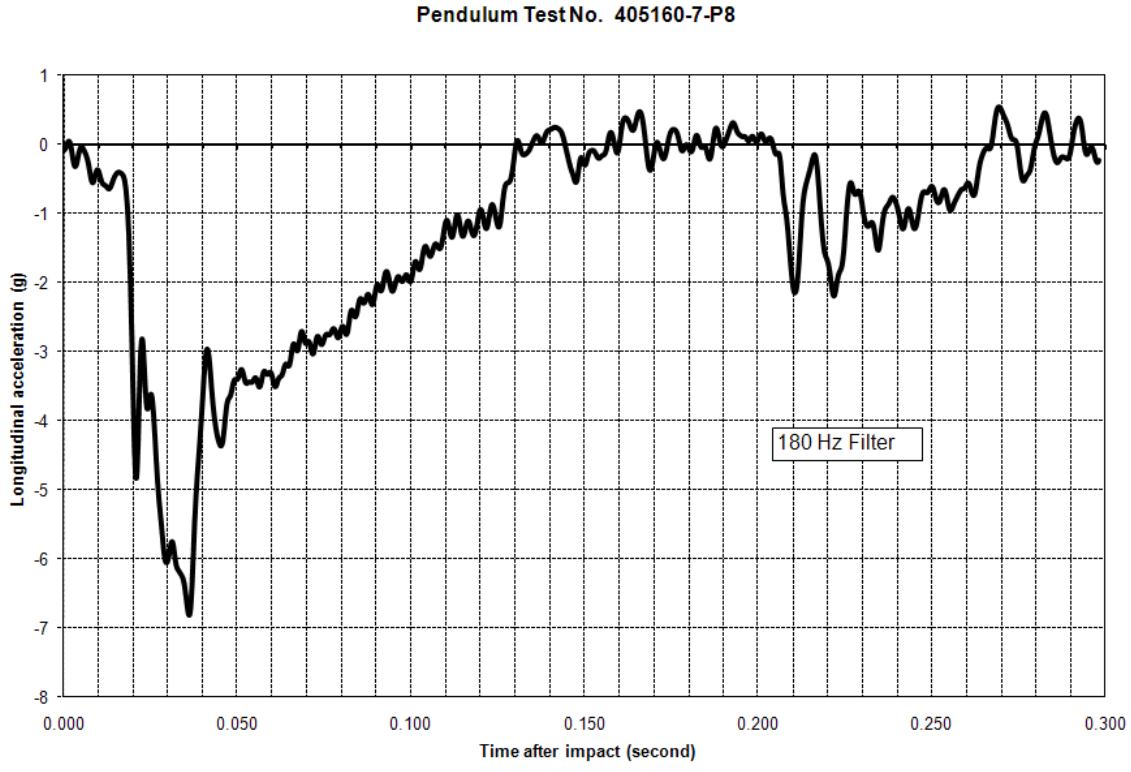

Figure B-11: Acceleration-time response from test P8.

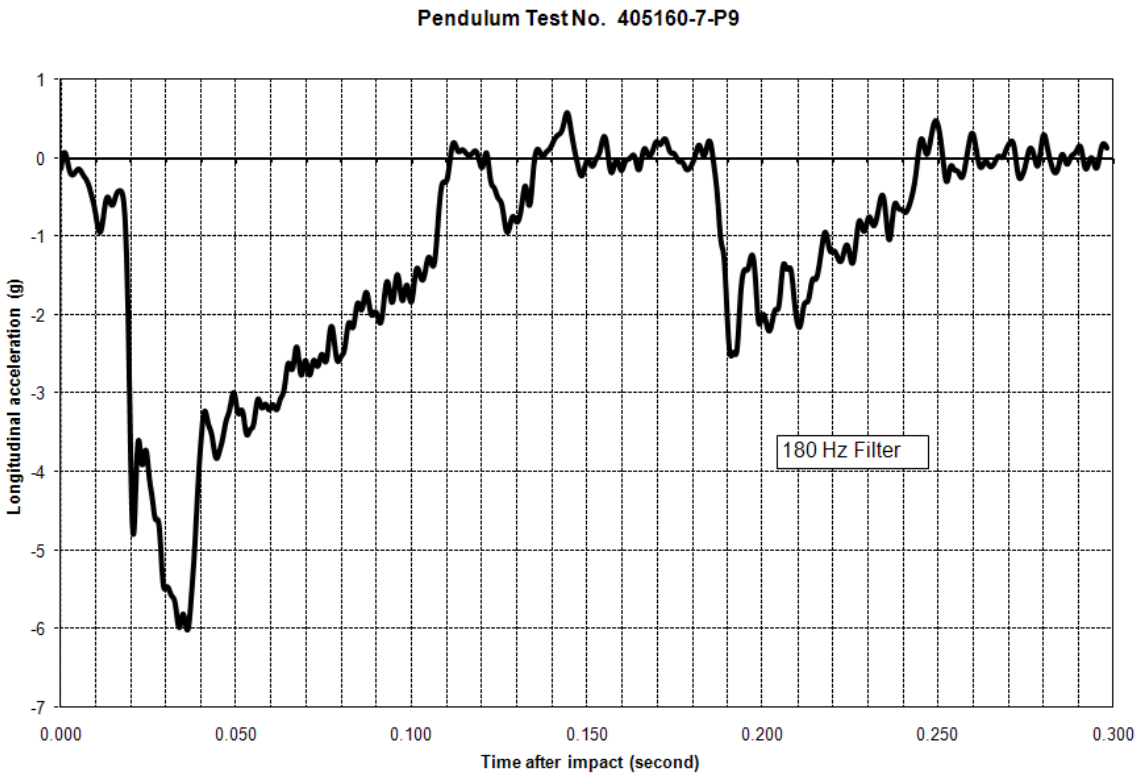

Figure B-12: Acceleration-time response from test P9.

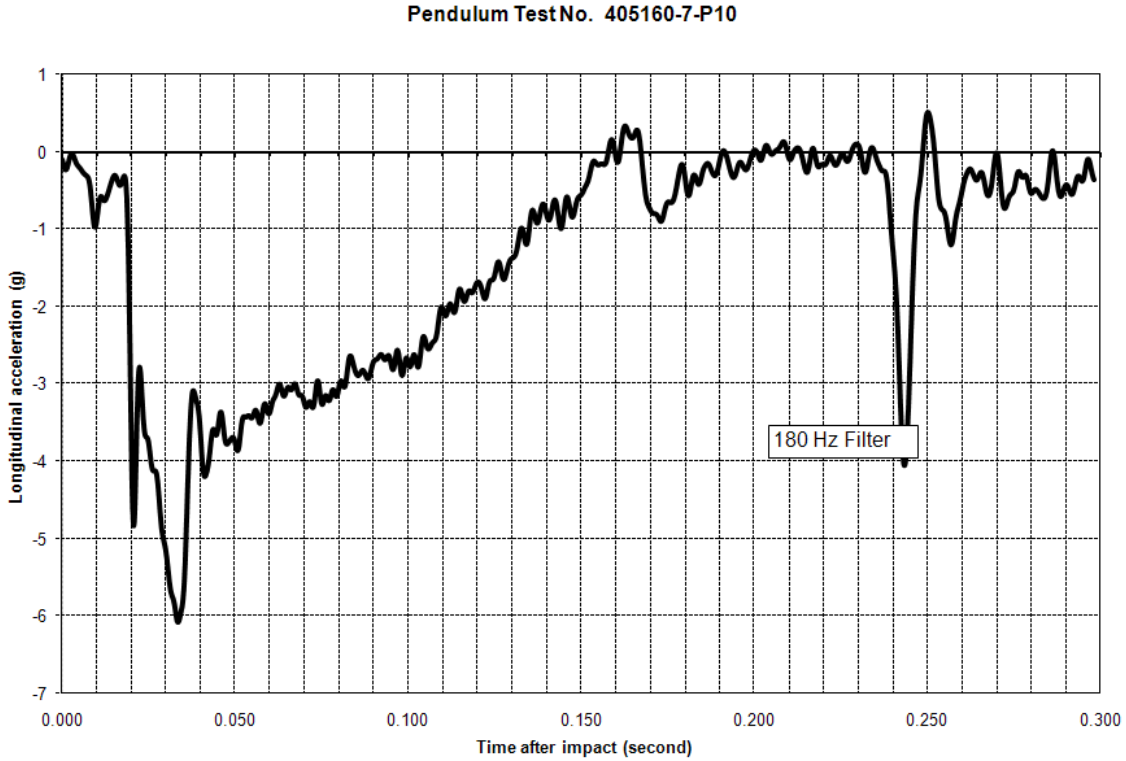

Figure B-13: Acceleration-time response from test P10.

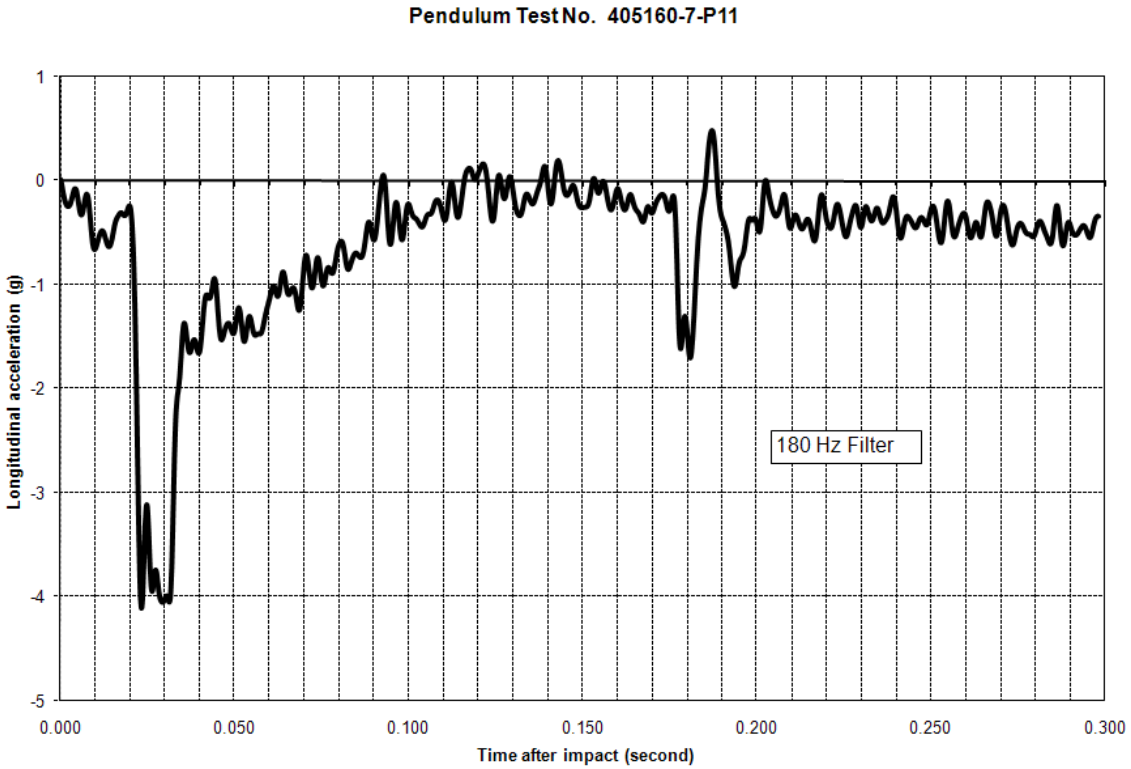

Figure B-14: Acceleration-time response from test P11.

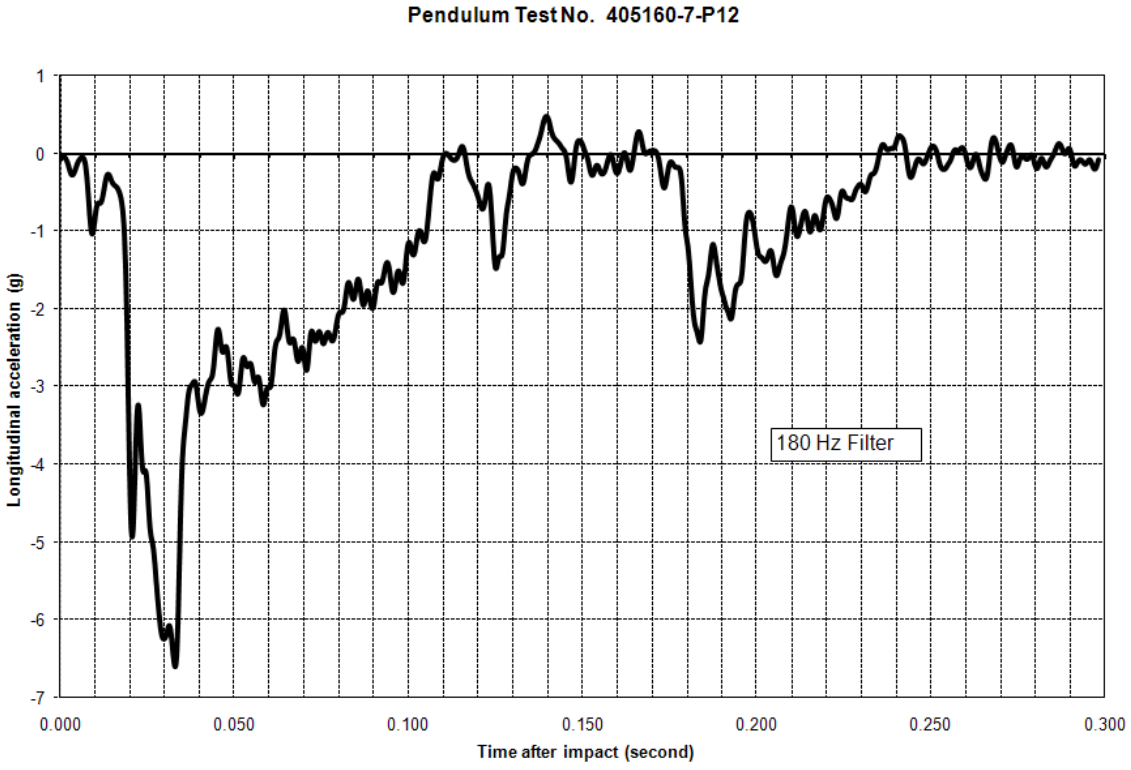

Figure B-15: Acceleration-time response from test P12.